

## Capacity and Earthquake Response Analysis of RC-Shear Walls



Bjarni Bessason  
Ph.D., Associate Professor  
Earthquake Engineering Research Centre, University of Iceland  
Austurvegur 2a, 800 Selfoss, Iceland  
E-mail: [bb@hi.is](mailto:bb@hi.is)



Thórdur Sigfússon  
M.Sc., Civil Engineer  
Faculty of Engineering, University of Iceland  
Austurvegur 2a, 800 Selfoss, Iceland  
E-mail: [thordur@vgs.is](mailto:thordur@vgs.is)

### ABSTRACT

The South Iceland Lowland is an active seismic zone. Approximately, 60% of all residential houses in the region are one or two stories reinforced-concrete buildings. In June 2000, two major earthquakes of magnitude 6½ struck the South Iceland. The earthquakes caused considerable damage, especially to older structures. No building collapsed, and no people suffered serious injuries. In this paper, a non-linear, finite-element model is calibrated by experimental data, and then used to evaluate the load-deformation curves of reinforced-concrete shear wall with different reinforcement configurations. The shear wall geometry is typical for Icelandic residential buildings. The evaluated load-deformation curves are then used in earthquake response analysis, using recorded strong motion data from the South Iceland earthquakes of June 2000.

**Key words:** Reinforced-concrete shear walls, non-linear pushover analysis, capacity curves, earthquake response.

## 1. INTRODUCTION

### 1.1 Background

The seismicity in Iceland is related to the Mid-Atlantic plate boundary crossing the island. Within Iceland, the boundary shifts eastward through two complex fracture zones. One is located in the South Iceland Lowland, called the South Iceland Seismic Zone (SISZ), while the other, lying mostly off the northern coast of Iceland, is called the Tjörnes Fracture Zone. The largest earthquakes in Iceland have occurred within these zones. The SISZ crosses the biggest agricultural region in Iceland. In this region, there are villages, schools, medical centres, industrial plants, hydro-electric power plants, and some major bridges. The population is around 16,000 inhabitants, and the number of residential houses is approximately 5,300. Most of the houses are low-rise buildings of one or two stories. Based on the official real property database, approximately 30% of all houses are wooden houses, 10% are masonry houses made of hollow

pumice blocks, and 60% are in-situ-cast concrete houses. The majority of the houses are built after 1940. In June 2000, two major earthquakes of moment magnitude  $M_w=6.6$  and  $M_w=6.5$  occurred in SISZ. No houses collapsed, but numbers of houses were damaged, and at least 35 houses were estimated as unrepairable and were renewed. Most of the damage was found in older shear-wall concrete and masonry buildings with poor reinforcement. In older houses reinforcement was usually just placed around window and door openings, and even only above the openings, see [1]. Figure 1 shows as an example of damage to two older houses during the South Iceland earthquakes of June 2000. It should be noted that the cracks are few but severe.

## 1.2 Objective

In this study, a finite element program is calibrated and verified against experimental data. Then the program is used to evaluate the capacity, represented by non-linear load-deformation curves, of reinforced-concrete shear wall with the same geometry but different reinforcement. The shear wall geometry is typical for Icelandic low-rise concrete residential houses. The capacity curves are then used as bases for non-linear earthquake response analysis of an idealised single-story residential building, which is excited by recorded acceleration time histories from the South Iceland earthquakes of June 2000. The main aim is to study the effect of different amounts of reinforcement on the capacity curves and to see if observed damage in the South Iceland earthquakes of June 2000 can be back-calculated.



*Figure 1 - Houses damaged during the South Iceland earthquakes of June 2000.*

## 2. NONLINEAR ANALYSIS OF REINFORCED CONCRETE

### 2.1 General

Non-linear response of reinforced concrete (RC) is caused by cracking, plastic deformations in compression and crushing of the concrete and plastic deformations of the reinforcement. Other, usually less important, time-independent non-linearity arises from bond slip between steel and concrete, aggregate interlock of cracked concrete and dowel action. Time-dependent effects, such as creep, shrinkage and temperature change, also affect non-linear response but can be ignored for short-duration earthquake loads. In the following, only non-linear properties due to cracking, plastic deformations of concrete and steel, and aggregate interlock are considered. A

perfect bond between the steel bars and the concrete is assumed, but according to [2], this assumption usually gives reasonably accurate results.

Many mathematical models have been proposed for non-linear finite element (FE) analysis of reinforced concrete structures. An overview of these models and how they can be modelled with the FE approximations can be found in [3] and [4].

A number of computer programs are available for non-linear analysis of reinforced concrete. The constitutive models and plasticity models used in these programs, however, are different, and it is generally not straightforward to apply these models. Some of the input parameters are fictive and have to be adjusted. In this work, the computer program ANSYS [5] is adapted and calibrated against experimental data.

## 2.2 Finite element model

The solid element SOLID65 in the ANSYS program is used in the analysis [5]. It can be used for three-dimensional modelling of solids with or without reinforcing bars. Eight nodes define the element, each having three translation degrees of freedom. Reinforcement can be defined in three different directions.

The solid part of the element, e.g., the concrete, is capable to describe cracking, plastic deformations and crushing. The plasticity model for concrete is based on the flow theory of plasticity, von Mises' yield criterion, isotropic hardening and associated flow rule, see [3]. Cracking is permitted in three orthogonal directions at each integration point. The cracking is modelled through an adjustment of the material properties (i.e., by changing the element stiffness matrixes) that effectively treat the cracking as “smeared” cracks. The concrete material is assumed to be initially isotropic. If the concrete at an integration point fails in uniaxial, biaxial, or triaxial compression, the concrete is assumed crushed at that point. Crushing is defined as the complete deterioration of the structural integrity of the concrete (e.g., concrete spalling).

The reinforcement is assumed smeared throughout the elements. An idealised elasto-plastic material model models the reinforcement. It cannot carry shear, i.e., transverse forces.

## 2.3 Input parameters

The following material parameters are necessary for the concrete model: uniaxial secant modulus of elasticity,  $E_c$ ; uniaxial secant modulus of plasticity,  $E_{cp}$ ; uniaxial compression strength,  $f_{cc}$ ; uniaxial tension strength,  $f_{ct}$ ; uniaxial yield strength,  $f_{cy}$ ; ultimate strain for concrete,  $\epsilon_{cu}$ ; shear coefficient for open crack,  $\beta_o$ ; shear coefficient for closed crack,  $\beta_c$ ; multiplier for tensile stress relaxation,  $T_c$ ; and finally Poisson's ratio,  $\nu_c$ . Some of the parameters have a clear physical meaning, while others are more fictive. The uniaxial stress-strain curve shown in Figure 2 can be used to explain some of the parameters above. However, the simple curve in Figure 2 is not representative of the general case of multiaxial stress state. In such cases, the curve is replaced by yield surfaces (von Mises) and fracture surfaces that are functions of principal stresses or principal-stress invariants, see [3] for more details.

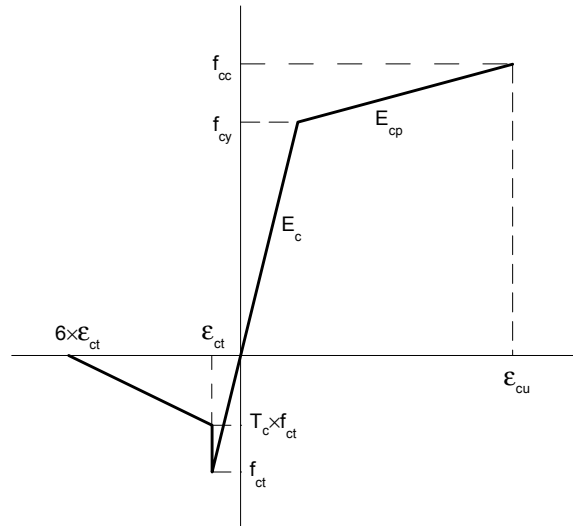


Figure 2 – Uniaxial concrete material model.

Based on studies presented by Hemmaty, see [2] and [6], it was decided to use  $\beta_c=1.0$  and  $\beta_t=0.1$  in all analyses. Furthermore, the default values,  $T_c=0.6$  and  $f_{cy}=0.8 \times f_{cc}$ , recommended in [5] and used in [2] and [6], were also used for all runs. The steel parameters are simpler and consist of: modulus of elasticity,  $E_s$ ; modulus of plasticity,  $E_{sp}$ ; yield strength,  $f_{sy}$ ; ultimate strain,  $\epsilon_{su}$ ; and, finally, Poisson's ratio  $\nu_s$ .

## 2.4 Verification against experimental data

Two laboratory-tested RC-beams and two laboratory-tested RC-walls were analysed with the computer program ANSYS [5]. The experimental data for the RC-beams were obtained from Bresler & Scordelis [7]. The beams were simply supported, 3660mm long, 305mm wide, 552mm high, and loaded with vertical force in the middle. Both beams had tension steel, but only one of the beams had shear reinforcement and compression steel in addition. Due to symmetry, only one half of the beam was modelled. Solid 3D elements were used: six elements in the height, two in the width and twelve in the length ( $6 \times 2 \times 12 = 144$ ). All physical input data (geometry, concrete and steel parameters) were according to the experimental data. In Figure 3, the experimental load-deflection curve for the beam with the shear reinforcement and the compression steel is compared with the FE-analysis curve. The load and the deflection shown are based on the applied force and the measured and computed deflection at the middle of the beam. As can be seen, the curves are quite similar. For more details, see [1].

The experimental data for the RC walls are obtained from Barda [8]. Laboratory tests of eight scaled, low-rise shear walls with boundary elements are described. All the shear-walls have the same geometry, but the reinforcement varies between the tests. The boundary elements were supposed to simulate the effect of cross walls and an overlying floor slab. The horizontal length of the test walls was 1910mm; the height was 610mm, and the thickness was 102mm. Only two tests were analysed with the ANSYS program. In Figure 4a the tilt-up from the laboratory tests [8] is shown, and in Figure 4b the FE-model of the test is shown. In Figure 5 the measured and computed load-deflection curves are shown for one of the shear walls. As can be seen, the FE-analysis can simulate the test results fairly well.

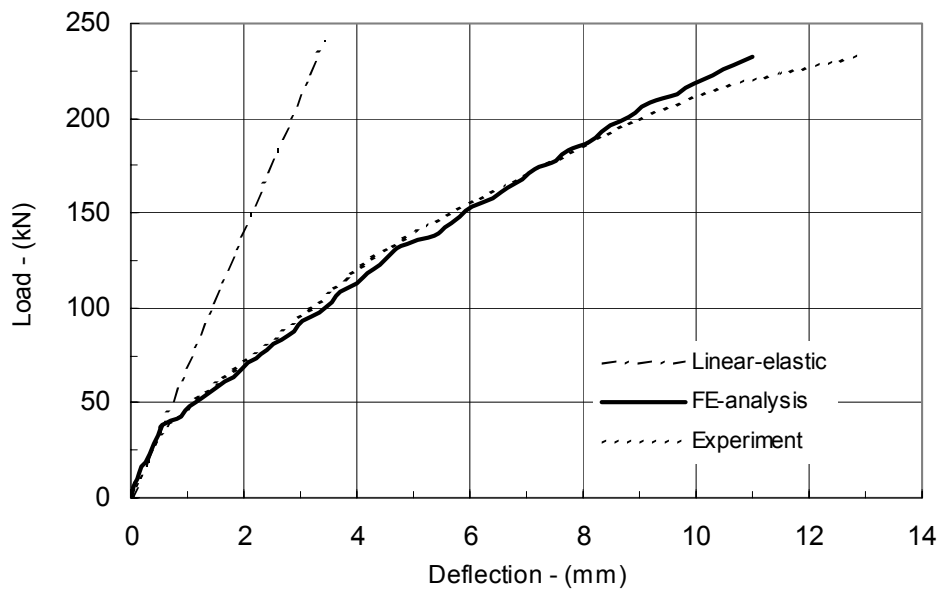


Figure 3 - Comparison of experimental [7] and FE-analysis [1] load-deflection curves for simply supported beam with shear reinforcement.

The main conclusion from the verification examples is that the FE-program can be used to simulate the whole load-deformation curve, i.e., the elastic part, the initiation of cracking, shear cracks and crushing, and the yielding of the steel bars fairly well. However, the determination of ultimate load is difficult as it is affected by the hardening rule, convergence criteria and iteration method used, [1]. It should be noted that each experiment considered was only based on one test, and no estimates for standard deviation or bonds of the results are available. It is likely that repeated tests would have resulted in some variations.

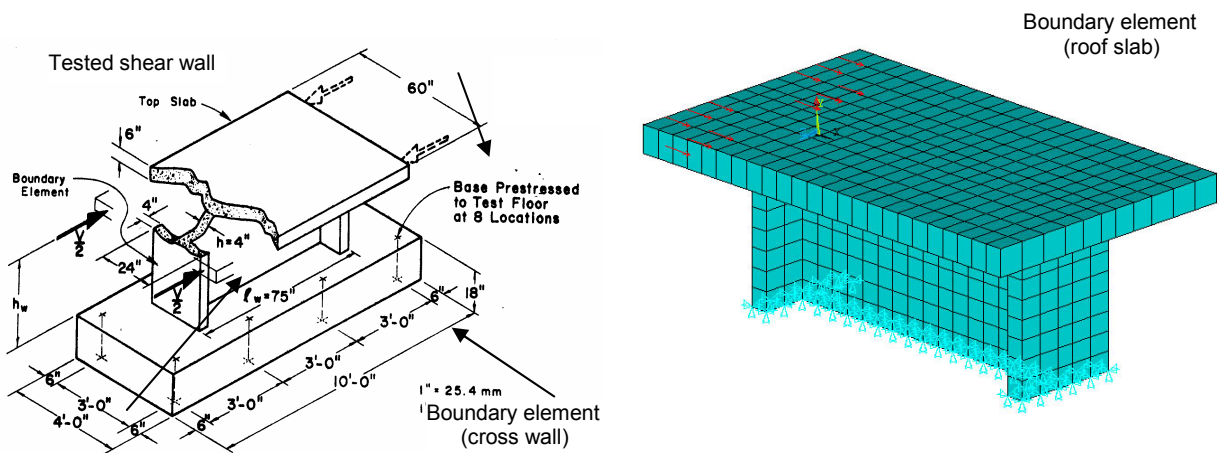


Figure 4 – a) Tilt-up of laboratory tested shear wall with boundary elements, from [8]. b) FE-model of the laboratory test from [1].

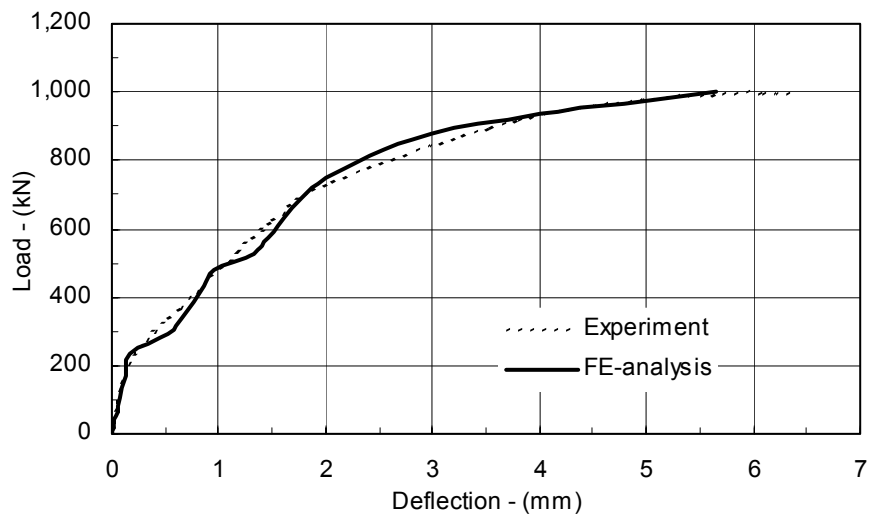


Figure 5 - Comparison of experimental [8] and FE-analysis [1] load-deflection curves for reinforced concrete shear wall with boundary elements.

### 3. PUSHOVER ANALYSIS OF LOW-RISE RC SHEAR WALL

#### 3.1 Typical residential concrete house

The capacity spectrum method used in the field of earthquake engineering compares the capacity of a structure with the demands of earthquake ground motion on it, see for instance [9] and [10]. The capacity of the structure is represented by a load-displacement curve, obtained by non-linear static analysis where the load is stepwise increased. This way of evaluating the load-displacement curve is often called a pushover analysis.

Approximately 60% of all residential houses in the South Iceland Lowland (SIL) are concrete buildings. In the period 1996-1997, a field survey was carried out in the SIL as a part of an earthquake mitigation program called SEISMIS, see [11]. The surveying procedure was based upon standardised questionnaires and inspection of architectural and engineering drawings. The field survey showed that concrete residential houses are usually one- to two-story shear-wall buildings, with 110-150m<sup>2</sup> living area and built after 1940. They are more or less symmetric, and most, and sometimes all, of the interior walls are non-bearing. The foundations are typically made of concrete with limited reinforcement and founded on rock or gravel. The exterior shear walls are typically 180mm thick. Concrete roof slabs are common, usually 150mm thick. In houses built before 1980, the concrete strength corresponds to approximately C16 concrete (characteristic compressive cylinder strength,  $f_{ck}=16\text{MPa}$ ), but in houses built after 1980, it normally corresponds to C20 concrete ( $f_{ck}=20\text{MPa}$ ), for more details see [12]. Today, only ribbed steel bars are used in concrete, but prior to 1965, plain steel bars were the only alternative. Before 1965, it was common to use only one or two horizontal, 12mm steel bars over window and door openings. Between 1965 and 1980, this reinforcement was increased to one or two 12mm steel bars around all openings. After 1980 the building authorities requested one layer of reinforcement grid in the entire wall. Normally, this was made of 10mm steel bars with a centre-to-centre (c/c) distance of 250mm in both the horizontal and vertical directions. After 1990, the reinforcement has increased, and it is now common to use double steel grid reinforcement, usually 2×(10 mm c/c 250mm).

In Figure 6 a concrete shear wall is defined that can be assumed to be representative of an exterior wall in a typical single-story residential house. This wall will be used in the pushover analysis. The wall is 0.18m thick, 8m wide and 2.75m high, with two windows and one door. Openings are 27% of the area, and the height to length ratio is 0.34. The geometry will be the same throughout the analysis, while the reinforcement configuration varies. The different reinforcement configurations are shown in Table 1. The steel type assumed is S400 ( $f_{sy}=400\text{MPa}$ ) in all cases, and the concrete strength corresponds to C20 concrete, see [12].

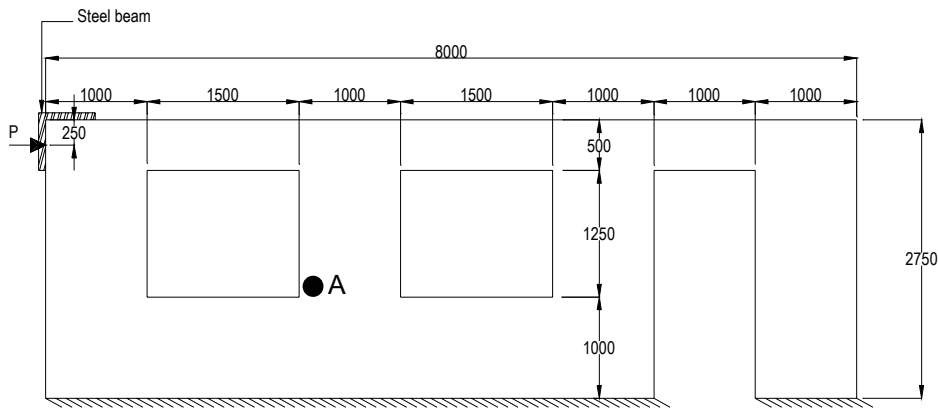


Figure 6 – Wall geometry used in pushover analysis. The reinforcement configuration is defined in Table 1. The dot to the right of the right window shows the location where the steel stresses are computed, in the diagram shown in Figure 9.

Table 1 - Reinforcement configuration used for the shear wall

Wall types	Reinforcement	$A_s/A_c$ vertical	$A_s/A_c$ horizontal
W1	No reinforcement	-	-
W2	1K12 around openings (1K12 - one 12 mm steel bar)	-	-
W3	2K12 around openings	-	-
W4	1K12 c/c250mm grid in the entire wall	0.25 %	0.25 %
W5	2K12 c/c250mm grid in the entire wall	0.5 %	0.5 %
W6	Minimum reinforcement according to Eurocode 2 (EC2) [12] without reinforcement around openings and boundary reinforcement.	0.4 %	0.2 %
W7	Minimum reinforcement according to EC2 with 2K16 around openings but no boundary reinforcement	0.4 %	0.2 %

### 3.2 FE-model

The shear wall is modelled with 256 solid elements (Solid65, see [5]). All the elements have the same size, i.e., height×width×thickness is 250×250×180mm. A steel square, modelled by linear beam elements, is put on the top left corner, where the load is applied, in order to distribute the load at the corner. It should be noticed that the element size might affect the results slightly, see for instance [13]. The Newton-Rapson iteration technique is used with displacement convergence criteria. The material properties for the concrete as well as the steel are based on mean values (expected values) and not on design values. For the concrete, the following values are used:  $E_c=28.8\text{MPa}$ ,  $E_{cp}=1.85\text{MPa}$ ,  $f_{cc}=25\text{MPa}$ ,  $f_{ct}=2.2\text{MPa}$ ,  $f_{cy}=0.8\times f_{cc}=20\text{MPa}$ ,  $\epsilon_{cu}=3.5\%$ ,

$\beta_l=0.1$ ,  $\beta_c=1.0$ ,  $T_c=0.6$ ,  $\nu_c=0.2$ . For the steel:  $E_s=200\text{GPa}$ ,  $E_{sp}=1.04\text{MPa}$ ,  $f_{sy}=400\text{MPa}$ ,  $\varepsilon_{su}=15\text{‰}$  and  $\nu_s=0.3$ . The horizontal load,  $P$ , is monotonic and applied stepwise at the top of the wall. In addition, the self-weight of the structure is included in the analysis, i.e., the dead load of the wall and the dead load of an idealised roof slab and roof structure supported by the wall.

### 3.3 Capacity curves

In Figure 7, the capacity curves for the wall types W2 to W7 are shown. The deflection shown is defined by the horizontal deflection at the top left corner.

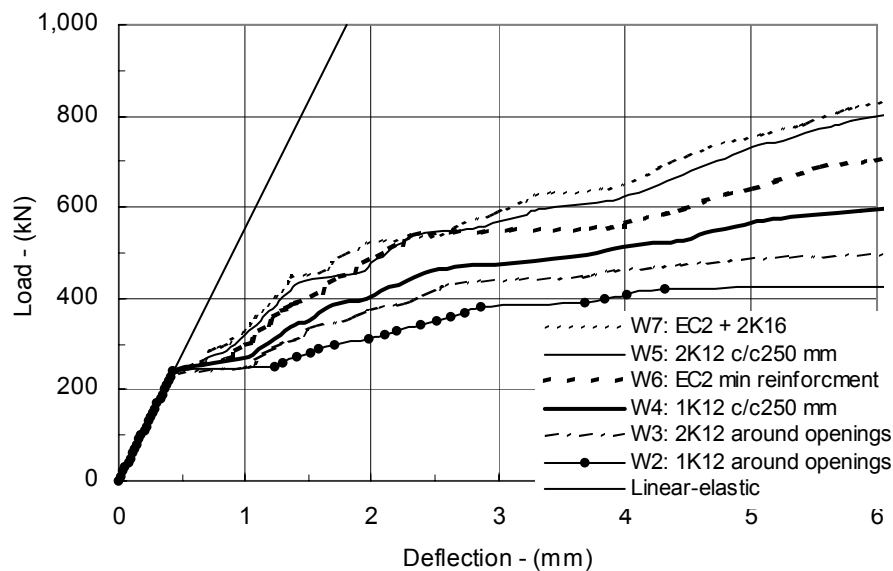


Figure 7 - Capacity curves for the shear wall with varying reinforcement.

In all the walls the initial cracking started at the load of 240kN and at a deflection of 0.44mm. Wall-W1 is not shown in the figure because it became unstable right after cracking. All curves have been cut off at deflection of 6mm although all wall types had higher ultimate displacement. This is done because at a displacement of 4mm, corresponding to a ductility of approximately  $\mu=8$ , it is expected that the structural stability of the walls is insufficient with buckling, brittle failure, etc., see for instance [14]. Walls with little reinforcement, i.e., walls W2 and W3, develop a kind of shear failure near initial cracking load. This can partly be seen in Figure 8 where the crack pattern in the W2-wall and the W7-wall is shown at a load of  $P=250\text{kN}$ , i.e., just after initial cracking. As seen, the W2-wall is cracked through the section, while only a few elements have cracked in the W7-wall. Due to the steel bars around the openings, the capacity of the W2-wall is nevertheless not exhausted. Here, as for the simulation of the experimental data, it is difficult to compute the ultimate load.

From Figure 8, it can also be seen that increasing reinforcement increases wall resistance. For instance, the W2-wall resists a load of approximately 410kN at a 4mm deflection. For the same deflection, the resisting load is 15%, 30%, 57%, 40% and 70% higher than this, for the W3-, W4-, W5-, W6- and W7-walls, respectively. In Figure 9, the steel stresses in the element to the right of the right window shown in Figure 6 (dot A) are shown as a function of deflection. From Figure 9, it can be seen, for example, that for the W2-wall the steel stresses at the observation point yield at approximately a 1.5mm deflection. For the W7-wall, the steel yields at the same point at a deflection of 5.5mm.

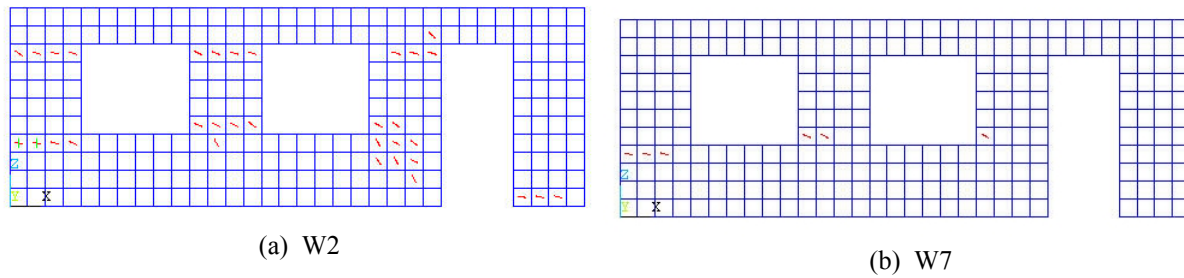


Figure 8 - Initial cracking in wall W2 and W7 at a load of 250kN.

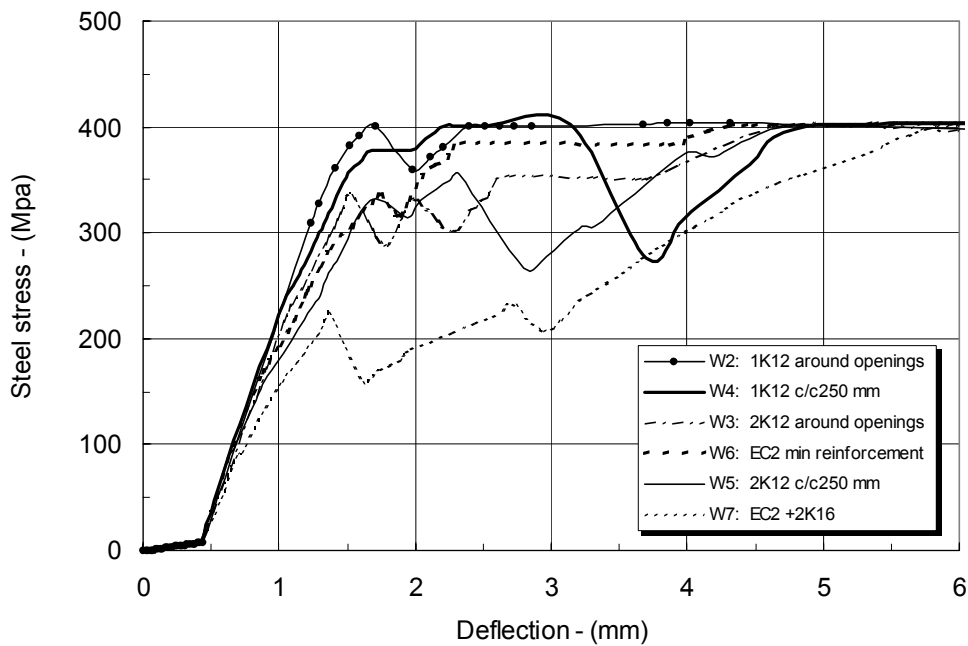


Figure 9 – Computed steel stresses at point A in Figure 6 for different reinforcement configurations as a function of deflection.

## 4. EARTHQUAKE RESPONSE

### 4.1 Tectonic

In June 2000, two major earthquakes occurred in the South Iceland Lowland (SIL). The first earthquake occurred on June 17, 2000, 15:41, (GMT). The moment magnitude has been estimated as  $M_w=6.6$ , the earthquake epicentre at  $63.97^\circ\text{N}$  and  $20.36^\circ\text{W}$  and the focal depth 6.3km, approximately. The second earthquake occurred on June 21, 2000, 00:52, (GMT). The moment magnitude has been estimated as  $M_w=6.5$ , the earthquake epicentre at  $63.97^\circ\text{N}$  and  $20.71^\circ\text{W}$ , and the focal depth as 5.3km, approximately. Observed surface fissures were found in a 20-25 km north-south elongated area in both earthquakes. Both events were right-lateral strike-slip earthquakes.

## 4.2 Strong motion records

The Earthquake Engineering Research Centre of the University of Iceland (EERC-UI) operates the strong motion network in Iceland. During the South Iceland earthquakes of June 2000, a number of records were recorded in the SIL. In the village Hella, with approximately 700 inhabitants, many houses were damaged in the first earthquake. The distance from the village to the closest surface fault rupture was only 2 to 3km. In this earthquake, the recorded horizontal peak ground acceleration (PGA) was 0.47g, see [15]. At the Kaldárholt Farm the residential house was damaged during the first earthquake and deemed un-repairable. The shortest distance between the farm and the surface fault rupture was 6km. The recorded PGA at the farm was 0.62g. In [15], elastic response spectra and constant-ductility response spectra for Hella and Kaldárholt are presented.

## 4.3 Earthquake response of residential houses

In this section the shear wall geometry used in the pushover analysis is assumed to be an exterior wall of an idealised 8×15m rectangular building with 150mm thick concrete roof slab. Furthermore, it is assumed that the lateral stiffness of the opposite exterior wall is identical, and that there are no parallel interior walls resisting lateral loads. Then the shear wall will resist 50% of the horizontal earthquake force in the longitudinal direction of the wall. It is estimated that the tributary weight of the roof slab and the roof structure, resisted by the shear wall, is 255kN, and that the half weight of the wall is 36kN, total  $W=291$ kN. Hence, most of the tributary weight is at the top of the shear wall. The wall can be assumed to resist earthquake forces as a single degree of freedom (SDOF) system, with the resisting forces defined by the capacity curves. This is shown schematically in Figure 10. For small earthquake loads, the wall would behave elastically, and for larger forces, exceeding the initial crack force, the wall would respond non-linearly. Using the initial stiffness of the system before cracking, the elastic natural period can be estimated from the capacity curve as:

$$T_E = 2\pi \sqrt{\frac{M}{F_Y / D_Y}} \quad (1)$$

where  $F_Y=240$ kN is the initial crack force;  $D_Y=0.44$ mm is the initial crack deflection;  $M=W/g$  is the tributary mass of the system, and  $g$  is the acceleration of gravity. Based on this, the elastic natural period is found to be  $T_E=0.046$ s. The so-called seismic coefficient,  $S_A(\xi, T_E)$ , where  $\xi$  is the damping ratio, and  $T_E$  is the elastic natural period of an SDOF-system, is a well-known parameter in the field of earthquake engineering, see for instance [16]. It is computed as a function of the two above parameters for a given acceleration time history, and presented in the form of so-called response spectra. Multiplying the mass of the SDOF-system by the seismic coefficient gives the maximum earthquake force on the system for the given acceleration time histories, i.e.:

$$F = M \cdot S_A(\xi, T_E) \quad (2)$$

For an appropriate damping ratio for the wall, the seismic coefficient has to be greater than  $F_Y/M=0.82g$  in order to initiate cracking and inelastic response of the walls. If the seismic coefficient is lower than this the wall will respond elastically and stay uncracked.

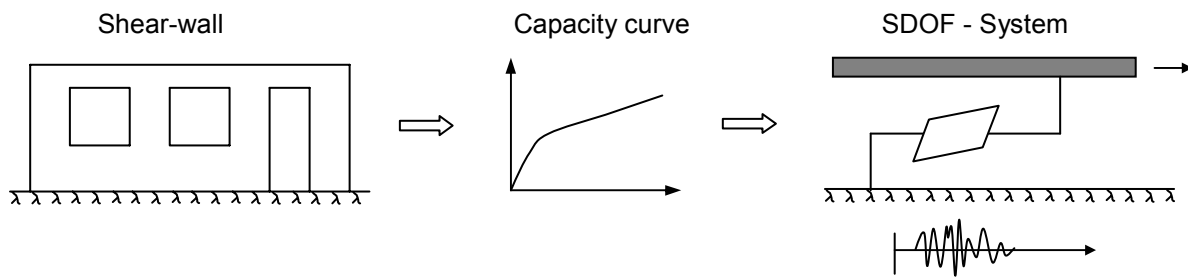


Figure 10 – Non-linear SDOF model of the shear walls, using the capacity curves to define the skeleton of the hysteresis rule.

In Figure 11, the linear elastic response spectra, for a 2% damping ratio is shown at the village Hella and at Kaldárholt Farm. The spectra are based on recorded acceleration time histories at these two sites during the South Iceland earthquake of June 17, 2000. Both components at each place are shown. The “crack point” for the shear walls ( $T_E = 0.046\text{s}$ ,  $S_A = 0.82\text{g}$ ) is also shown on the plot.

According to Figure 11, the shear wall would have behaved elastically at Hella during the June 17, earthquake, even if it had been unreinforced. However, it should be kept in mind, as can be seen in [1], that walls with weaker concrete, i.e., C16, which is common in older houses, are more flexible and have a lower yield point. Further, more unfavourable wall geometries, i.e., more openings, also, reduce its capacity.

If the wall would have been in Kaldárholt, see Figure 11, then the earthquake forces would have exceeded the elastic capacity of the wall, and yielding of the wall would have occurred. This would have been the case for both the horizontal components of the earthquake. The inelastic earthquake response of the walls can be estimated by using the capacity curves to define the skeleton of a hysteresis rule for the SDOF-system, and then by using time-history analysis and step-by-step integration [9]. Below, this method is applied to the W2- and W7-walls, using the N-S acceleration time histories from Kaldárholt as excitation, see Figure 12.

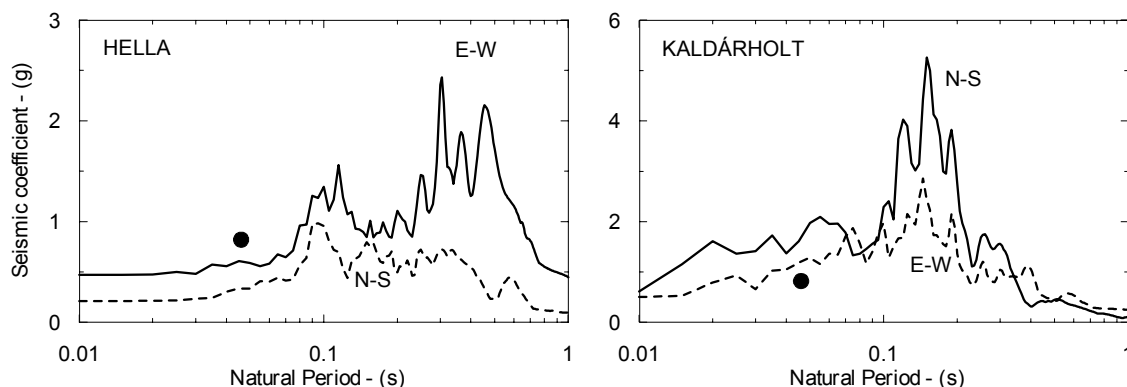


Figure 11 - Linear elastic response spectra with 2% damping ratio at Hella and Kaldárholt, based on the South Iceland earthquake of June 17, 2000. Both the horizontal components are shown. The dot shows the crack point for the shear wall in Figure 6.

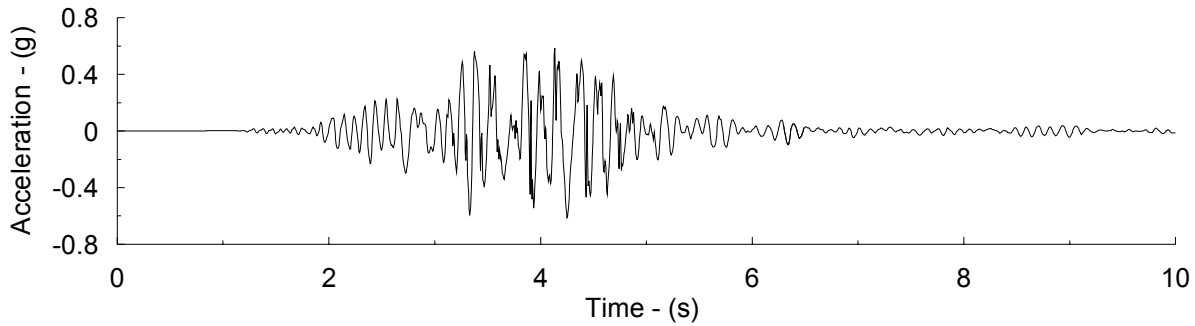


Figure 12 – The recorded N-S acceleration component in Kaldárholt during the South Iceland Earthquake of June 17, 2000.

In Figure 13, the W2 and W7 capacity curves have been fitted by bilinear curves. These curves are used to define a bilinear hysteresis rule for the system, see Figure 10. The program Ruaumoko [17] is used for the analysis. The results are given in Table 2. The calculated deflections are low and do not exceed the limits of the bilinear curve in Figure 12, meaning that the bilinear fit is acceptable. The results indicate that the wall type W7 would have resisted the severe earthquake excitation in Kaldárholt with low ductility demand,  $\mu=1.7$ , and limited cracking. The pushover analysis, showed that for this ductility, the steel stresses are about 50% of the steel yield stress, see Figure 9. On the other hand, the W2-wall only has reinforcement around openings, and as soon the wall cracks, they will very probably be severe. Recalling from Figure 5 that for  $P=250\text{kN}$ , it should be noted that the cracks in the W2-wall already stretched between the openings. In the above, no attempt has been made to consider the effect of cumulative damage and strength degradation due to the cycling earthquake load.

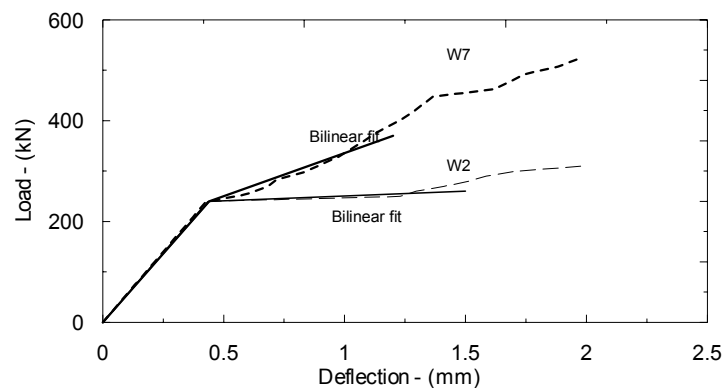


Figure 13 - Capacity curves for shear walls W2 and W7 from Figure 7 fitted with bilinear curves.

Table 2 - Earthquake response of the W2 and W7-walls, modelled by bilinear SDOF-system and excited by the recorded N-S acceleration component from Kaldárholt in the South Iceland earthquake of June 17 2000.

Wall types	Maximum deflection	Ductility demand	Shear force	Seismic coefficient
W2	0.97 mm	2.1	249 kN	0.86 g
W7	0.76 mm	1.7	296 kN	1.02 g

## 5. SUMMARY AND CONCLUSIONS

Nonlinear pushover analysis was carried out for low-rise, reinforced, concrete shear walls with openings. All the walls had the same type of concrete and geometry but different reinforcement configurations. The reinforcement varied from none to Eurocode 2 minimum requirements with extra reinforcements around openings. The results clearly indicate that changing the reinforcement greatly affects the capacity of the walls. The analysis indicated that all the walls crack at the same load level. Walls with little reinforcement developed shear failure just after the initial crack load. The crack widths were not evaluated, but it is likely that these cracks are open and severe as soon as they form. Such severe cracks were observed in the damaged houses with poor reinforcement in the South Iceland earthquakes of June 2000. The model showed that well reinforced shear walls distributed the cracks over a greater area than the poorly reinforced walls, and these cracks are generally more closed, especially when the steel is below the yield point. The analysis also indicated that the capacity of the shear wall is highly affected by the reinforcement around the openings.

Two of the analysed shear walls were assumed to be an exterior wall in a single story, 120-m<sup>2</sup> residential house with a roof slab. One of the walls had poor reinforcement, while the other was properly reinforced. The walls were supposed to resist 50% of the lateral earthquake load on the house in the longitudinal direction of the walls. From the capacity curve, the so-called crack point could be found, defined by the elastic natural period and the crack capacity of the walls. This crack point was then compared with the elastic demand spectra developed from the South Icelandic earthquakes of June 17, 2000. The response spectra were based on recorded data from the Kaldárholt Farm and the village of Hella. In both these places, severe damage was experienced during the June 17 earthquake. The comparison indicated that the crack limits for the walls was not exceeded at Hella. In Kaldárholt the crack limits were exceeded, and the walls would be subjected for inelastic response. Nonlinear dynamic analysis indicated that the poorly reinforced wall would probably be seriously damaged in the June 17 earthquake, while the more properly reinforced walls would have resisted the severe earthquake excitation with minor or no damage. When evaluating the results, it should be kept in mind, that the concrete strength in the analysis was relatively high with respect to the older buildings. Furthermore, mean values were used in the analysis, and strength distribution and/or degradation were not considered.

The study shows that nonlinear pushover analysis is a realistic and reliable method for evaluating the structural response of reinforced concrete structures in seismic zones. In further studies, shear walls with different geometries, reinforcement layout and material properties should be analysed as well as existing walls that failed in the South Iceland earthquakes of June 2000. Furthermore, the method can be used in the design of new structures and in repairing and retrofitting structures as well as in code calibration and risk assessment.

## ACKNOWLEDGEMENTS

The Icelandic Concrete Association supported this work. This support is gratefully acknowledged

## REFERENCES

1. Sigfússon Th., *Nonlinear analysis of reinforced concrete shear walls in low-rise Icelandic residential Buildings*, Master Thesis, University of Iceland, 2001.
2. Hemmaty, Y., De Roeck G., Vandewalle, L. & Mortelmans, F., Parametric study of RC corner joints subjected to positive bending moment by a nonlinear FE Model, *ANSYS Conference*, Pittsburgh, PA, 1992.
3. Chen, W.F. *Plasticity in reinforced concrete*, John Wiley & sons, Inc, New York, 1982.
4. ASCE Committee 447 on finite element analysis of reinforced concrete. *State-of-the-art report on finite element analysis of reinforced concrete*, American Society of Civil Engineering (ASCE), 1982.
5. ANSYS Engineering Analysis System. *User and Theoretical Manual*. ANSYS, Inc. Southpointe, Canonsburg, Pennsylvania, Version 5.6.2, 1998.
6. Hemmaty Y. Modeling of the shear force transferred between cracks in reinforced and fibre reinforced concrete structures, *ANSYS Conference*, Pittsburgh, PA, 1998.
7. Bresler, B. & Scordelis, A.C., *Shear strength of reinforced concrete beams*, Institute of Engineering research, University of California Berkeley, California, 1964.
8. Barda, F., *Shear strength of low-rise walls with boundary elements*, Ph.D. Thesis, Lehigh University, Bethlehem, Pennsylvania, 1972.
9. Fajfar. P., Capacity spectrum method based on inelastic demand spectra, *Earthquake Engineering and Structural Dynamics*, 1999; 28(9): 979-93.
10. Chopra, A.K. & Rakesh K.G, Capacity-demand-diagram methods based on inelastic design spectrum, *Earthquake Spectra*, 1999; 15(4): 637-56
11. Sigbjörnsson, R., Bessason, B., Sigfússon, Th.I., Sigfússon, Th., & Thorvaldsdóttir, S., Earthquake risk mitigation in South Iceland, *Proceedings of the Eleventh European Conference on Earthquake Engineering*, Balkema, Rotterdam, 1998.
12. CEN, *Eurocode 2 – Design of concrete Structures – Part 1: General rules and rules for buildings*, (ENV 1992-1-1), CEN, Berlin, 1991
13. Shayanfar, M.A., Element size effects in nonlinear analysis of reinforced concrete members. *Computers & Structures*, 1997; 62(2); 339-52.
14. Paulay, T. & Priestley M.J.N., *Seismic Design of Reinforced Concrete and Masonry Buildings*, John Wiley & Sons, Inc., New York, 1992.
15. Sigbjörnsson, R., Snaebjörnsson, J., Ólafsson, S., Bessason, B., Baldvinsson, G.I. & Thórarinnsson, Ó., *Earthquakes in South Iceland*, Report no. 0001, Earthquake Engineering Research Centre, University of Iceland, 2000 (written in Icelandic).
16. Chopra, A., *Dynamics of Structures: Theory and Application to Earthquake Engineering*, Prentice-Hall, 2<sup>nd</sup> ed., 2000.
17. Carr, J., *Ruaumoko – program for inelastic dynamic analysis*, University of Canterbury, 1981-2000.